

# Antibiofouling Slippery Liquid Impregnated Pulsed Plasma Poly(styrene) Surfaces

Joe M. Rawlinson, Harrison J. Cox, Grant Hopkins, Patrick Cahill, and Jas Pal S. Badyal\*

**Biofouling is a major global environmental and economic challenge wherein organisms settle on solid surfaces submerged in natural waters. This leads to the spread of invasive marine species around the globe, accelerates surface deterioration through microbially-induced corrosion, and inflates maritime vessel fuel consumption which leads to greater greenhouse gas emissions. In this study, pulsed plasma poly(styrene) nanocoatings impregnated with eco-friendly liquids are produced that yield slippery surfaces through aromatic–aliphatic intermolecular interactions (water droplet contact angle hysteresis and sliding angle values  $\approx 1\text{--}2^\circ$ ). The antibiofouling performance of these slippery surfaces is demonstrated using laboratory-based marine bioassays and real-world field trials in freshwater (pond water) and seawater (ocean) environments. Low-cost and substrate-independent pulsed plasmachemical deposition combined with eco-friendly liquid impregnation provides a sustainable approach to tackling environmental biofouling.**

hydrodynamic drag increasing vessel fuel consumption to generate higher greenhouse gas emissions.<sup>[4,5]</sup>

Liquid-repellent surfaces inspired by the *Nepenthes* pitcher plant (which entraps liquid within a textured surface to capture arthropod prey) have previously been fabricated through liquid impregnation of roughened or porous surfaces.<sup>[6–10]</sup> Careful matching of the solid and impregnation liquid chemistries can produce stable tightly bound slippery fluidic film at the substrate surface (water droplet contact angle hysteresis and sliding angle values  $\approx 1\text{--}5^\circ$ ).<sup>[11]</sup> This retained liquid film acts as a physical barrier preventing direct contact of chemical or biological moieties with the solid underlying material<sup>[12]</sup>—blocking the attachment


## 1. Introduction

The settlement and growth of microscopic and macroscopic organisms on solid surfaces submerged in seawater (marine biofouling) is a major challenge for maritime industries due to its multitude of negative impacts, including: facilitating the spread of invasive species around the globe (considered a major threat to the conservation of biodiversity in the world's oceans),<sup>[1]</sup> accelerated deterioration of surfaces through microbially-induced corrosion,<sup>[2]</sup> added biofoulant weight causing mechanical stresses on static structures,<sup>[3]</sup> and greater

of biofouling organisms (antibiofouling) and providing protection against corrosion (anticorrosion).<sup>[13–17]</sup> Other technological applications for slippery liquid-impregnated surfaces include water repellency,<sup>[18]</sup> icephobicity,<sup>[19]</sup> antifogging,<sup>[20]</sup> fog harvesting,<sup>[21,22]</sup> biomedical applications,<sup>[23,24]</sup> and drag reduction.<sup>[25–27]</sup> For marine antibiofouling applications, these systems offer great promise given that the incompressible trapped liquid layers are resistant toward changes in hydrostatic pressure (a common flaw of trapped gas layers within superhydrophobic structures).<sup>[10,28–31]</sup> Superhydrophobic surfaces are also susceptible to failure due to gas diffusion from the trapped gas layer into the surrounding water, and contamination by low surface tension oils—which is not an issue for slippery surfaces impregnated with water immiscible liquids.<sup>[29,32]</sup>

However, previous liquid-impregnated slippery surfaces have been reliant upon roughened or porous substrates which limits their more widespread application with respect to the range and geometries of suitable materials (due to the substrate-dependence of roughening or creation of porosity). Whereas the plasmachemical approach is substrate-independent (due to inherent electrical discharge activation of the substrate) and therefore more widely applicable. Surface roughness can also accelerate biofouling due to microscopic organisms preferentially settling into microtextures to maximize the interfacial contact area for adhesion.<sup>[33–36]</sup> Furthermore, many liquid-impregnated surfaces displaying marine antibiofouling properties utilize environmentally harmful synthetic/fluorinated oils.<sup>[16,37–41]</sup> Although eco-friendly liquids such as oleic acid and natural blackseed oil

J. M. Rawlinson, H. J. Cox, J. P. S. Badyal  
 Department of Chemistry  
 Science Laboratories  
 Durham University  
 DH1 3LE Durham, UK  
 E-mail: j.p.badyal@durham.ac.uk  
 G. Hopkins, P. Cahill  
 Cawthron Institute  
 Nelson 7010, New Zealand

 The ORCID identification number(s) for the author(s) of this article can be found under <https://doi.org/10.1002/admi.202300284>

© 2023 The Authors. Advanced Materials Interfaces published by Wiley-VCH GmbH. This is an open access article under the terms of the Creative Commons Attribution License, which permits use, distribution and reproduction in any medium, provided the original work is properly cited.

DOI: 10.1002/admi.202300284

impregnated into suitable solid substrates have been shown to reduce the settlement of marine biofouling organisms (such as mussels), they still require large quantities of solvent or multi-step, complex, and lengthy fabrication techniques.<sup>[42,43]</sup> Likewise, slippery non-porous/untextured polydimethylsiloxane (PDMS) surfaces impregnated with fluorinated oils, silicone oils, or ionic liquids have been reported for marine antibiofouling applications;<sup>[15,44–48]</sup> but the adherence of low surface energy bulk PDMS coatings are limited to specific types of underlying substrate, as well as inherent non-biodegradability, and multi-step, complex and lengthy coating procedures.<sup>[49–51]</sup>

Plasmachemical deposition has previously been used to produce liquid-impregnated porous coatings for slippery applications.<sup>[52,53]</sup> More recently, slippery surfaces have been fabricated utilizing favorable intermolecular aromatic–aliphatic interactions, for example between pulsed plasma deposited poly(styrene) nanocoatings and impregnated oils.<sup>[54–56]</sup> Aromatic–aliphatic liquid impregnated slippery surfaces negate the requirement for porous structures associated with conventional SLIPS (Slippery Liquid Infused Porous Surfaces), which can be costly and complex to fabricate. Key advantages of pulsed plasmachemical deposition include rapid single-step, ambient conditions, solventless, 3D conformal coatings, substrate-independent, strong adhesion, low energy consumption, minimal waste products, and industrial scalability.<sup>[57–61]</sup>

In this article, pulsed plasma poly(styrene) nanocoatings are impregnated with a variety of liquids to create aromatic–aliphatic interaction slippery liquid-repellent surfaces, **Figure 1**. Environmentally friendly liquids utilized in this study include squalane (which can be easily derived from olive oil or sugar cane),<sup>[62,63]</sup> and essential oils (2-methylundecanal and decanal) found in the peel of various fruits.<sup>[64,65]</sup> Other impregnation liquids tested include hexadecane (non-polar) and 1-undecanol (polar) which are commonly used as food flavorings,<sup>[66,67]</sup> and readily available mixtures of commercial oils (olive oil, rapeseed oil, and mineral oil). Antibiofouling tests have been conducted on these pulsed plasma poly(styrene)-impregnated liquid surfaces in natural pond water and the ocean.

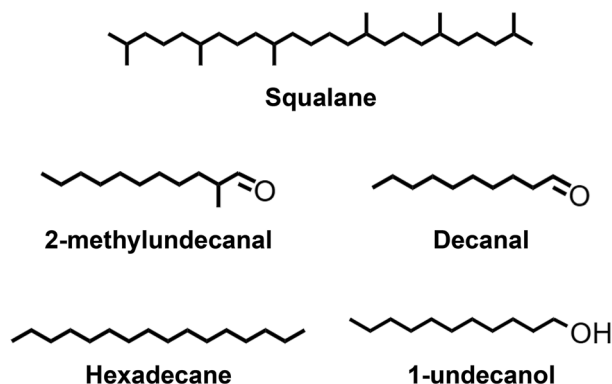


**Figure 1.** Chemical structures of impregnation liquids used to produce slippery surfaces on pulsed plasma poly(styrene) nanocoatings. Olive oil, rapeseed oil, and mineral oil are not shown given that they are mixtures of chemical structures.

## 2. Experimental Section

### 2.1. Pulsed Plasmachemical Deposition

A cylindrical glass reactor (5.5 cm diameter, 475 cm<sup>3</sup> volume, base pressure <math>2 \times 10^{-3}</math> mbar, and air leak rate better than  $6 \times 10^{-9}</math> mol s<sup>-1</sup>) housed within a Faraday cage was used for plasmachemical deposition.<sup>[58,68]</sup> The reactor was attached to a rotary pump (model E2M2, Edwards Vacuum Ltd.) via a liquid nitrogen cold trap. A copper coil wound around the reactor (4 mm diameter, 10 turns, located 6 cm downstream from the gas inlet) was connected to a custom-built 13.56 MHz radio frequency (RF) power supply via an inductance–capacitance (L–C) matching network to minimize the standing wave ratio for power transmission. An external pulse signal generator was used to trigger the RF power supply. Prior to each plasmachemical deposition, the reaction chamber was thoroughly scrubbed with hot water and detergent, rinsed with propan-2-ol (+99.5%, Fisher Scientific UK Ltd.) and acetone (+99%, Fisher Scientific Ltd.), and oven dried at 150 °C for at least 1 h, followed by 50 W continuous-wave air plasma cleaning at 0.2 mbar for 30 min. Poly(ethylene terephthalate) (PET, 50 mm × 80 mm, Mylar A 125, DuPont Teijin Films UK Ltd.) and Petri dish (Part no. Titan-02048493, Shanghai Titan Scientific Co. Ltd.) substrates were cleaned by placement into a 50/50 v/v solvent mixture of hexane (+99.5%, Fisher Scientific UK Ltd.) and propan-2-ol for 15 min and then dried in air at ambient temperature for at least 30 min. Silicon wafers (orientation: <math>\langle 100 \rangle</math>, resistivity: 5–20 Ω cm, thickness:  $525 \pm 25</math> μm, front surface: polished, back surface: etched, Silicon Valley Microelectronics Inc.) substrates were cleaned by sonication in a 50/50 v/v solvent mixture of hexane and propan-2-ol for 15 min and then dried in air at ambient temperature for at least 30 min. Cleaned substrates were then placed into the center of the plasma chamber copper coils and the system was pumped to base pressure. Styrene monomer precursor (+99%, Sigma-Aldrich Ltd.) was loaded into a sealable glass tube, degassed via multiple liquid nitrogen freeze–pump–thaw cycles, and attached to the plasma reactor. Monomer vapor was then allowed to purge through the system at a pressure of 0.2 mbar for 10 min followed by electrical discharge ignition. An initial 40 W continuous wave plasma was run for 5 s and then switched to pulsed mode conditions ( $P_{\text{on}} = 40</math> W;  $t_{\text{on}} = 100</math> μs;  $t_{\text{off}} = 4</math> ms) for 10 min. Upon extinction of the electrical discharge, the monomer vapor was allowed to continue to pass through the system for a further 10 min before the chamber was evacuated to base pressure and vented to atmosphere.$$$$$

### 2.2. Liquid Impregnated Slippery Surfaces

Oils for impregnation into the pulsed plasma poly(styrene) nanocoatings were selected according to their chemical structures to match aromatic–aliphatic intermolecular interactions (aliphatic containing groups) and physical properties (low volatility and water immiscibility): squalane (96%, Sigma-Aldrich Ltd.), 2-methylundecanal (>98%, Mystic Moments Madar Corporation Ltd.), decanal (>98%, Mystic Moments Madar Corporation Ltd.), hexadecane (99%, Sigma-Aldrich Ltd.), 1-undecanol (98%, Arcos Organics brand, Fisher Scientific UK Ltd.), olive oil (Olive oil, Tesco plc.), rapeseed oil (Vegetable oil, Tesco plc.), and mineral

oil (HE-175 Vacuum Pump Oil, Leybold Vacuum Products Inc.), Figure 1. Substrates were submerged into neat liquid at room temperature for 15 min. They were then carefully removed from the liquid using tweezers, placed into 50 mL of deionized water, and shaken vigorously for 5 min. Finally, the samples were dried in air for at least 3 h in a vertical orientation to allow any remnant excess liquid to drip off the surface onto tissue paper.

### 2.3. Surface Characterisation

#### 2.3.1. Infrared Spectroscopy

Fourier transform infrared (FTIR) analysis of pulsed plasma poly(styrene) surfaces was carried out using an FTIR spectrometer (model Spectrum One, Perkin Elmer Inc.) equipped with a liquid nitrogen-cooled mercury–cadmium–telluride (MCT) detector. The spectra were averaged over 100 scans at a resolution of  $4\text{ cm}^{-1}$  across the  $450\text{--}4000\text{ cm}^{-1}$  wavenumber range. Attenuated total reflectance (ATR) infrared spectra were obtained using a diamond ATR accessory (model Golden Gate, Graseby Specac Ltd.). Reflection–absorption (RAIRS) measurements utilized a variable-angle accessory (Graseby Specac Ltd.) fitted with a KRS-5 polarizer (to remove the *s*-polarized component) set at  $66^\circ$  to the surface normal.

#### 2.3.2. Coating Thickness

Pulsed plasma polymer coating thickness was measured using a spectrophotometer (model nkd-6000, Aquila Instruments Ltd.). Transmittance–reflectance spectra ( $350\text{--}1000\text{ nm}$  wavelength range and a parallel (*p*) polarized light source at a  $30^\circ$  incident angle) were acquired and fitted to a Cauchy model for dielectric materials using a modified Levenberg–Marquardt algorithm (version 2.2 software, Pro-Optix, Aquila Instruments Ltd.).<sup>[69]</sup> 10 min of pulsed plasma poly(styrene) deposition onto silicon wafers yielded an average thickness of  $262 \pm 86\text{ nm}$  (deposition rate =  $8.7 \pm 2.9\text{ nm min}^{-1}$ ). This value was calculated using ( $n = 6$ ) coated silicon wafer substrates and the standard deviation was taken for the error value.

A mass balance (model AJ 150 L, Mettler-Toledo LLC.) was used to weigh pulsed plasma poly(styrene) coated PET film before and after squalane liquid impregnation (rinsed in high-purity water and dried). The thickness of the impregnated liquid layer was calculated using the measured increase in mass, the wetted area, and the density of squalane ( $0.81\text{ g cm}^{-3}$ ).<sup>[70]</sup> The thickness of the impregnated squalane liquid layer on pulsed plasma poly(styrene) was calculated to be  $1.9 \pm 0.2\text{ }\mu\text{m}$ —this value was comparable to previously reported values for slippery surfaces which had been prepared using alternative methods.<sup>[10,71]</sup> Measurements were made for at least three ( $n = 3$ ) separate samples and the calculated standard deviation for the error value.

#### 2.3.3. Atomic Force Microscopy

Atomic force microscopy (AFM) images were obtained using a scanning probe microscope (Peakforce QNM mode, model Mul-

tiMode 8-HR, Bruker Corp.). Scans with at least 256-line resolution were acquired using AFM probes with a nominal force constant of  $0.4\text{ N m}^{-1}$  (ScanAsyst Air, Bruker Corp.) operating at a cantilever frequency of 1 kHz in the vertical direction. Nanoscope analysis v1.50 software was employed for image processing including second-order polynomials to remove natural curvature due to sample movement relative to the cantilever. Surface roughness measurements were calculated from at least three ( $n = 3$ ) samples with the standard deviation taken for the error value.

#### 2.3.4. Water Repellency

Water contact angle measurements at  $20\text{ }^\circ\text{C}$  used high-purity water (BS 3978 grade 1) and a video contact angle goniometer fitted with a motorized syringe (VCA 2500 XE, AST Products Ltd.). A  $2.0\text{ }\mu\text{L}$  water droplet was used for the static contact angle value. Dynamic contact angle values were measured by increasing the dispensed  $2.0\text{ }\mu\text{L}$  water droplet by a further  $2.0\text{ }\mu\text{L}$  at a rate of  $0.1\text{ }\mu\text{L s}^{-1}$  (advancing) and then subsequently decreasing the droplet volume by  $2.0\text{ }\mu\text{L}$  at a rate of  $0.1\text{ }\mu\text{L s}^{-1}$  (receding).<sup>[72]</sup> Droplet images were analyzed using ImageJ software in conjunction with the Dropsnake plugin.<sup>[73]</sup> Static and dynamic water contact angle values were calculated from measurements taken on at least three or more random locations on each of three ( $n = 3$ ) separate samples, and the average standard deviation was taken for the error value. No significant difference in water contact angle or water contact angle hysteresis values were measured for control or squalane-impregnated pulsed plasma poly(styrene) coated PET using larger ( $8\text{ }\mu\text{L}$ ) droplets, Table S1 (Supporting Information).

Water droplet sliding angle measurements were undertaken at  $20\text{ }^\circ\text{C}$  using a V-block adjustable angle gauge (model Adjustable Angle Gauge/Tilting Vee Blocks small, Arc Euro Trade Ltd.). This entailed fixing samples onto the tilt stage at an initial angle of  $0^\circ$  and dispensing a  $50\text{ }\mu\text{L}$  droplet onto a random point of the surface. The inclination of the stage was then slowly increased by  $1^\circ$  every 15 s until the water droplet movement was observed.<sup>[74]</sup> The measurements were repeated on three separate samples ( $n = 3$ ) and the standard deviation was taken as the error value.

### 2.4. Antibiofouling Testing

#### 2.4.1. Natural Pond Water

Preliminary antibiofouling performance of liquid-impregnated pulsed plasma poly(styrene) surfaces was assessed locally within the UK by placement into an outdoor plastic tank (volume =  $115\text{ L}$ , temperature range:  $12\text{--}20\text{ }^\circ\text{C}$ ) which had been filled with natural water collected from a nearby pond and fitted with two metal rods to suspend samples, Figure S1 (Supporting Information). The water temperature at a depth of  $\approx 15\text{ cm}$  was monitored using a thermometer. Algal growth was sustained by adding  $15\text{ mL}$  of water-soluble fertilizer (Miracle-Gro All Purpose Plant Food, Scotts Miracle-Gro Co.) to the biofouling tank water every two weeks.<sup>[75]</sup>

Samples were fixed in plastic projector slide mounts ( $70\text{ mm} \times 70\text{ mm}$ , part no. M-9425, Matin International Co.) and attached

to the top of a plastic box (model no. HPL822B, Locknlock Co.) to form a sample–mount–box assembly in which samples could be held horizontally in the water, Figure S1 (Supporting Information). Samples were photographed at the beginning of the experiment (12-megapixel, model A1688, Apple Inc.), and the sample–mount–box assembly was then submerged into the pond water tank at a depth of  $\approx 15$  cm for 7 days. After removal from the tank, the sample–mount sections were detached from the plastic box and gently dipped twice into fresh tap water to remove any unadhered fouling material from the surface and photographed again.

A colorimeter (model PCE-CSM 4, PCE Instruments UK Ltd.) was used to measure the color of the surfaces before (pristine) and after pond submersion to provide a rapid quantitative measure of outdoor biofouling accumulation onto surfaces, with larger color changes indicating greater levels of adhered fouling biological material.<sup>[76,77]</sup> Color measurements of each sample were taken both before and after pond water submersion under fixed lighting conditions with a constant backing color. The color change was calculated for the CIELAB color space using Equation (1), where  $L^*$  is the lightness of the color,  $a^*$  is the position between red and green, and  $b^*$  is the position between blue and yellow.<sup>[78]</sup> The measurements were repeated at least three times ( $n \geq 3$ ) at random locations for each sample and the standard deviation was taken as the error value.

$$\Delta E = \sqrt{\Delta L^{*2} + \Delta a^{*2} + \Delta b^{*2}} \quad (1)$$

#### 2.4.2. Marine Bioassay

Subsequently for the best performing natural pond water antibiofouling samples, bioassays were undertaken using pulsed plasma poly(styrene) coated Petri dish substrates (Part no. Titan-02048493, Shanghai Titan Scientific Co. Ltd.) impregnated with squalane (slippery behavior was re-confirmed after transportation of samples from UK to New Zealand, by water droplets rapidly rolling off the coated substrate). These experiments took place in a purpose-built chamber that consisted of a polyethylene tub (30 cm wide, 30 cm long, 15 cm deep) with horizontal rails on two of the vertical sides, Figure S2 (Supporting Information). These rails held a polycarbonate backing plate to which three ( $n = 3$ ) replicate treated Petri dish samples and three ( $n = 3$ ) control Petri dishes (untreated polystyrene, Corning CoStar) were affixed using adhesive Velcro dots. The slippery samples and controls were randomly arranged on the backing plate.

The samples were assessed for antibiofouling activity against three model biofouling taxa: the Pacific transparent sea squirt (*Ciona savignyi*), the blue mussel (*Mytilus galloprovincialis*), and the blue tubeworm (*Spirobranchus caraniferus*). Broodstock of these species sourced from coastal populations in the Nelson region of New Zealand were held in a recirculating seawater system ( $18.0 \pm 1.0$  °C,  $33 \pm 1$  PSU) and fed bulk cultured *Isochrysis galbana* until ready to spawn. Spawning and larval culture followed previously described methodologies.<sup>[79–81]</sup> Larval competence was assessed prior to experiments as follows: *Ciona savignyi* – the species was lecithotrophic and competent to settle upon hatching.<sup>[79]</sup> *Mytilus galloprovincialis* – during larval culture, larvae were inspected daily to assess developmental stage; larvae are

considered competent to settle when they reach the “pediveliger” stage and had developed a functional foot and eye spot ( $\approx 18$ – $20$  days post fertilization).<sup>[82]</sup> *Spirobranchus caraniferus* – during larval culture, larvae were inspected daily to assess body size; larvae were considered competent to settle when they reached 300–330  $\mu\text{m}$  body length ( $\approx 15$  days); due to the conspecific settlement characteristic of this species, fully grown larvae were then exposed to  $10^{-3}$  M 3-isobutyl-1-methylxanthine for 4 h immediately prior to use in the experiment to induce settlement.<sup>[83]</sup> During experiments, the competence of larvae was assessed directly via the controls (i.e., the settlement of larvae on the blank controls demonstrated that the larvae were competent to settle).

Competent larvae of each species were used separately in bioassays to quantify settlement and adherence to the liquid-impregnated pulsed plasma poly(styrene) coatings. In each instance, the bioassay chamber was filled with seawater, and  $\approx 5000$  larvae were added. The chamber was left for 5 days ( $18.0 \pm 1.0$  °C,  $33 \pm 1$  PSU, 12 h:12 h light:dark). After 5 days, the backing plate with attached samples was removed from the chamber and the number of larvae that had successfully settled and attached to each sample and control Petri dish were counted using a binocular microscope. For any larvae that did attach to the liquid-impregnated surface, their attachment structures were inspected visually for differences in appearance relative to larvae on the control surfaces using a compound microscope (Olympus CKX41, Olympus, Japan). For *C. savignyi*, the surface area of attachment structures was measured using image analysis software (CellSens, Olympus) and compared using two-tailed t-tests. Measurement did not occur for *S. caraniferus* because no larvae settled on the squalane surface (therefore, there was nothing to measure). Measurement of attachment area for *M. galloprovincialis* was technically not possible at the settlement stage because they attach by mucous threads, which were diffuse and highly transparent.

#### 2.4.3. Marine Field Trial

Pulsed plasma poly(styrene) coated Petri dish substrates impregnated with squalane (slippery behavior was re-confirmed by water droplets rapidly rolling off the substrate) were deployed in Nelson Marina, Nelson, New Zealand ( $-41.258996^\circ$  S,  $173.281478^\circ$  E) from 25/10/22 to 8/12/22 to determine antibiofouling efficacy in the marine environment, Figure 2. Three ( $n = 3$ ) squalane-impregnated pulsed plasma poly(styrene) coated substrates and three ( $n = 3$ ) control substrates (untreated polystyrene, Corning CoStar, Sigma-Aldrich Ltd.) were affixed in a random arrangement to a 1 m<sup>2</sup> polycarbonate backing plate using adhesive Velcro dots. The backing plate was immersed upside down  $\approx 1.5$  m below the ocean surface. After 2, 4, and 6 weeks, the plate was retrieved and a high-resolution photograph was taken of each Petri dish. These images were analyzed for percentage cover of biofouling using Coral Point Count (CPCe V4.1).<sup>[84]</sup> Each image had 25 points overlaid in a stratified random design. Each point was assessed visually and assigned as “bare space” (i.e., no visible biofouling), “biofilm”, or a macrofouling organism. The latter were identified to the lowest possible taxonomic resolution (species level in many instances) but data were pooled to “Bryozoans”,





**Figure 2.** Location of test samples in Nelson Marina, Nelson, New Zealand ( $-41.258996^{\circ}$  S,  $173.281478^{\circ}$  E) from 25/10/22 to 8/12/22 to determine antibiofouling efficacy in the marine environment.

“Filamentous seaweeds”, “Hydroids”, and “Ascidians” for calculation of percentage cover.

The deployment occurred during austral spring (see dates above) when biofouling pressure (inoculation) was significant and increased at the study location. The timing of this deployment during spring was considered to be a “hard” test of the squalane-impregnated pulsed plasma poly(styrene) coating’s performance.

### 3. Result

#### 3.1. Infrared Spectroscopy

Liquid styrene monomer exhibits the following characteristic infrared absorption bands: C–H stretching ( $2965\text{--}3100\text{ cm}^{-1}$ ), aromatic ring summations ( $1700\text{--}2000\text{ cm}^{-1}$ ), vinyl C=C stretching ( $994$  and  $1629\text{ cm}^{-1}$ ), and aromatic ring stretching ( $1451$ ,  $1492$ , and  $1600\text{ cm}^{-1}$ ), **Figure 3**. Pulsed plasma deposited poly(styrene) retains the aforementioned aromatic ring features, whilst disappearance of the vinyl band absorbances confirms that high selectivity plasmachemical polymerization of styrene has taken place via the opening of the vinyl carbon–carbon double bond.

#### 3.2. Coating Surface Morphology

Atomic force microscopy (AFM) analysis showed that the pulsed plasma poly(styrene) nanocoatings were smooth ( $\text{Roughness}_{\text{RMS}} = 0.83 \pm 0.50\text{ nm}$  for  $5\text{ }\mu\text{m} \times 5\text{ }\mu\text{m}$  scan area) and large scale porosity was absent, **Figure S3** (Supporting Information). This lack of surface roughness is consistent with aromatic–aliphatic intermolecular interactions underpinning the observed slippery behavior.

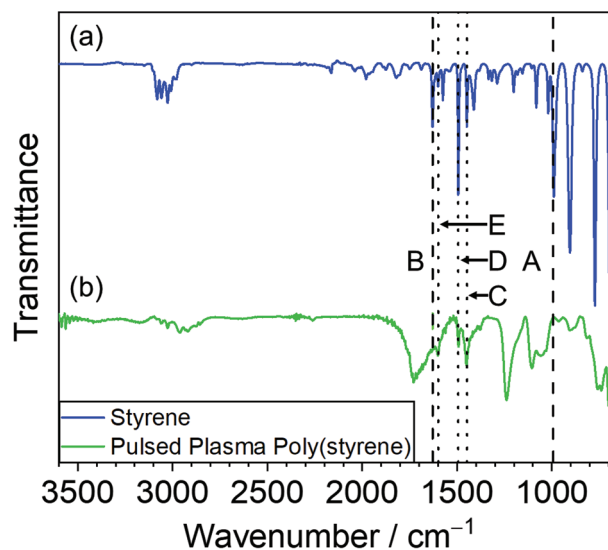


**Figure 3.** Infrared spectra of a) styrene monomer (ATR); and b) pulsed plasma poly(styrene) films deposited onto a silicon wafer (RAIRS). Vinyl group absorbances (dashes:  $A = 994\text{ cm}^{-1}$  and  $B = 1629\text{ cm}^{-1}$ ); and aromatic ring absorbances (dots:  $C = 1451\text{ cm}^{-1}$ ,  $D = 1492\text{ cm}^{-1}$ , and  $E = 1600\text{ cm}^{-1}$ ).

#### 3.3. Water Repellency

Pulsed plasma poly(styrene) coatings display a higher water contact angle value, and lower water contact angle hysteresis and sliding angle values compared to uncoated PET substrate, **Figure 4**. Liquid impregnation into the pulsed plasma deposited poly(styrene) nanocoating gave rise to slippery behavior (water contact angle hysteresis and sliding angle values  $< 5^{\circ}$  for

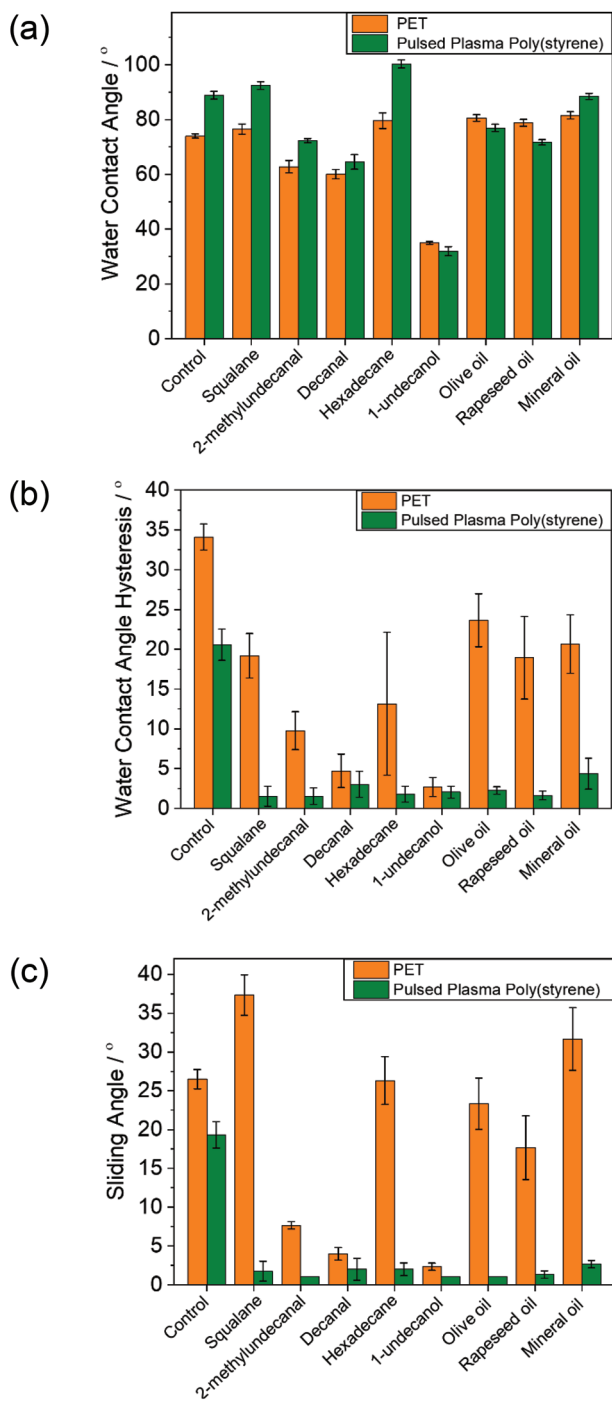


**Figure 4.** Water repellency of control PET and pulsed plasma poly(styrene) coated PET substrates following impregnation with a variety of liquids: a) water droplet contact angle; b) water droplet contact angle hysteresis; and c) water droplet sliding angle (Table S2, Supporting Information). Mean values ( $n \geq 3$ )  $\pm$  average standard deviation.

a wide range of liquids (squalane, 2-methylundecanal, decanal, hexadecane, 1-undecanol, olive oil, rapeseed oil, mineral oil). These low water contact angle hysteresis and sliding angle values can be attributed to the favorable aromatic surface–aliphatic oil molecular interactions which underpin slippery behavior. For

the control PET substrate, slippery behavior was only observed for decanal and 1-undecanol, Figure 4. Water droplets did not slide readily over uncoated PET substrate, whilst easily glided at low inclinations over the surface of squalane-impregnated pulsed plasma poly(styrene) coated PET, Supporting Information Videos S1 and S2.

### 3.4. Biofouling

#### 3.4.1. Natural Pond Water

Submersion of pulsed plasma poly(styrene) coated PET substrate (control) in pond water for 7 days gave rise to light green algal material adhered to the surface, **Figure 5**.

Compared to the pulsed plasma poly(styrene) coated PET substrate (control), an increase in surface biofouling was observed for slippery pulsed plasma poly(styrene) impregnated with four of the liquids (decanal, 1-undecanol, olive oil, and rapeseed oil). Hexadecane impregnated into pulsed plasma poly(styrene) crystallized upon submersion into natural pond water and therefore was not investigated further (surface color changed from clear to white, 18 °C melting point of hexadecane compared to the

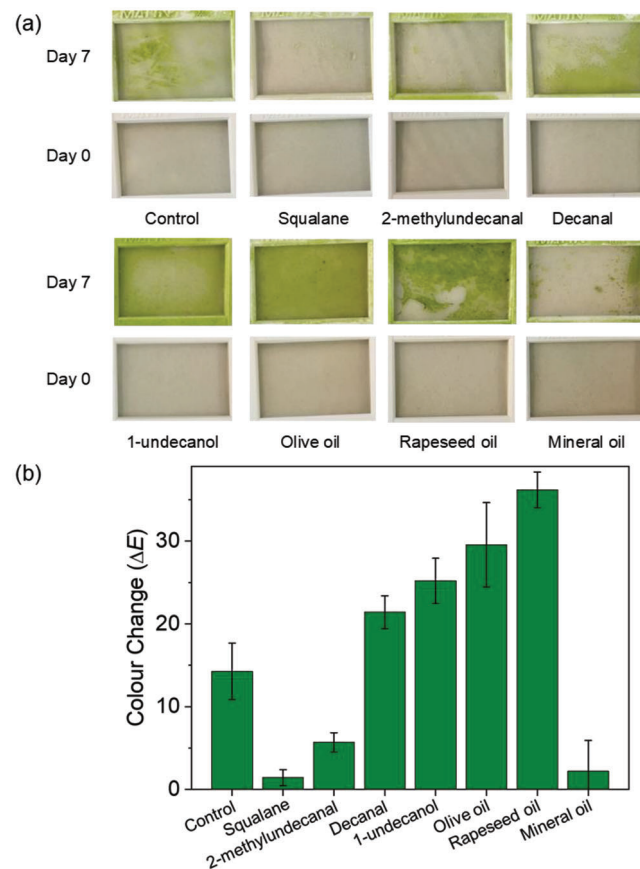


**Figure 5.** Pulsed plasma poly(styrene) coated PET impregnated with various liquids before and after 7 days of submersion in natural pond water: a) photographs; and b) color change ( $\Delta E$ ). Control corresponds to no liquid impregnation into pulsed plasma poly(styrene) coated PET. Mean values ( $n \geq 3$ )  $\pm$  average standard deviation.

pond water temperature of 12–20 °C).<sup>[85]</sup> A relative reduction in surface biofouling was noted for three of the impregnated liquids (squalane, 2-methylundecanal, and mineral oil), Figure 5. Squalane-impregnated pulsed plasma poly(styrene) coated PET gave rise to the lowest color change value ( $\Delta E = 1.4 \pm 1.0$ ), following 7 days of submersion into pond water.

Following 7-day pond water submersion, the water contact angle value for the control pulsed plasma poly(styrene) coated PET substrate (no liquid impregnation) decreased significantly (from  $88 \pm 1^\circ$  to  $46 \pm 8^\circ$ ), whilst water contact angle hysteresis and sliding angle values increased—this can be attributed to biofoulants adhering to the surface, Figure 6.<sup>[86]</sup> For the liquid-impregnated pulsed plasma poly(styrene) coated PET surfaces which had displayed lower color change (antibiofouling) compared to the control sample (squalane, 2-methylundecanal, and mineral oil, Figure 5), smaller water contact angle hysteresis and sliding angle values were retained after 7 days submersion into pond water, Figure 6. The extremely low water solubility of these hydrocarbon oils prevents their dissolution into the surrounding water, thereby creating a stable slippery interface deterring biofouling.<sup>[87]</sup> Squalane-impregnated pulsed plasma poly(styrene) coated PET surfaces exhibited the lowest water droplet contact angle hysteresis and sliding angle values following 7-day pond water submersion—which correlates to its best performance for natural pond water antibiofouling, Figure 5.

### 3.4.2. Marine Bioassay

The best performing antibiofouling surface identified for pond water (squalane-impregnated pulsed plasma poly(styrene) nanocoating) was tested further against selected model marine fouling organisms. Larval settlement rates were high on the control uncoated Petri dishes, Figure 7. By comparison, very few larvae settled and attached to the slippery squalane-impregnated pulsed plasma poly(styrene) coated Petri dishes. *S. caraniferus* larvae did not adhere to the squalane-impregnated samples, representing 100% antifouling efficacy against this taxon. A few *C. savignyi* and *M. galloprovincialis* larvae attached to the squalane-impregnated samples yielding antifouling efficacy exceeding 97% for both taxa. For the latter, any attached larvae were observed in discrete clusters near the edge of only one of the three replicate Petri dishes for each taxon (*C. savignyi* and *M. galloprovincialis*). When attachment structures were inspected and measured for *Ciona savignyi*, there were no detectable differences in the surface area or visual morphology between the squalane coating and controls, thereby confirming non-toxicity, Table S3 (Supporting Information). Attachment structures were not quantified for *M. galloprovincialis* due to their attachment mechanism via mucous threads, which is technically difficult to visualize.

### 3.4.3. Marine Field Trial

Control samples developed extensive biofouling coverage within 2 to 4 weeks of submersion in the ocean, with relatively uniform biofilm layers succeeded by macrofouling communities comprising filamentous seaweeds, hydroids, and bryozoans, Figure 8.

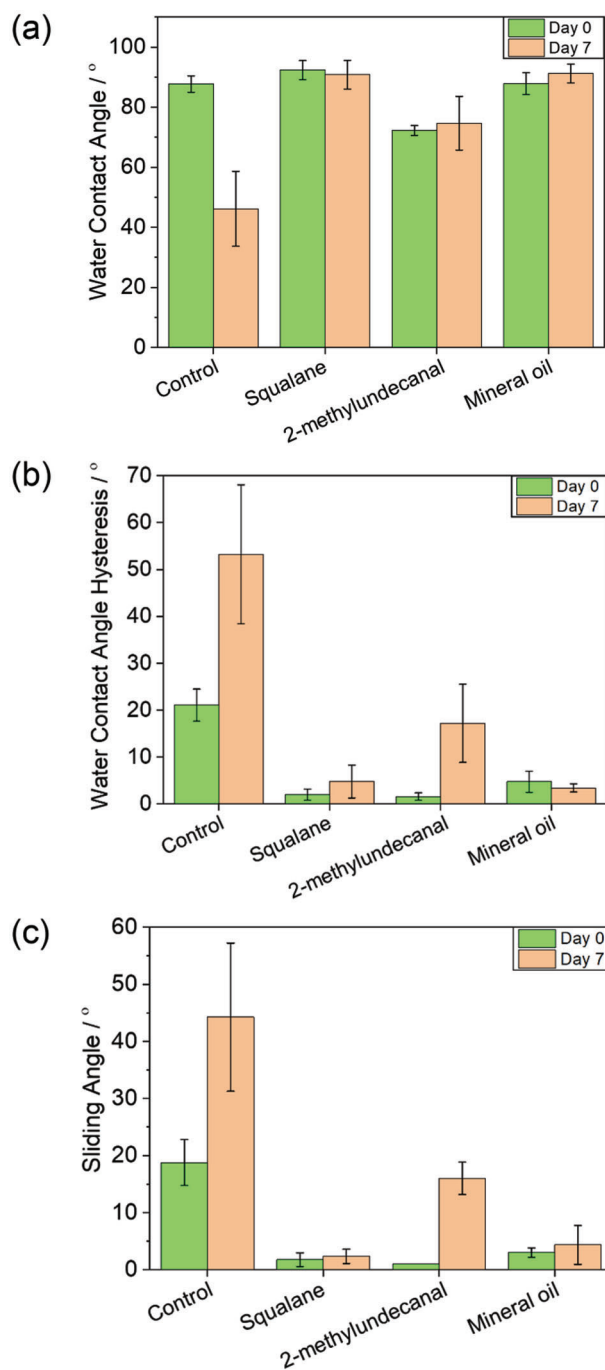


**Figure 6.** Antibiofouling pulsed plasma poly(styrene) coated PET impregnated with various liquids (squalane, 2-methylundecanal, and mineral oil) before and after submersion in natural pond water for 7 days: a) water droplet contact angle; b) water droplet contact angle hysteresis; and c) water droplet sliding angle. Control corresponds to no liquid impregnation into pulsed plasma poly(styrene) coated PET. Mean values ( $n \geq 3$ )  $\pm$  average standard deviation.

By comparison, biofouling development was strongly inhibited for at least 6 weeks on pulsed plasma poly(styrene) coated Petri dishes impregnated with squalane—thereby demonstrating the durability of the slippery coatings in real-world ocean



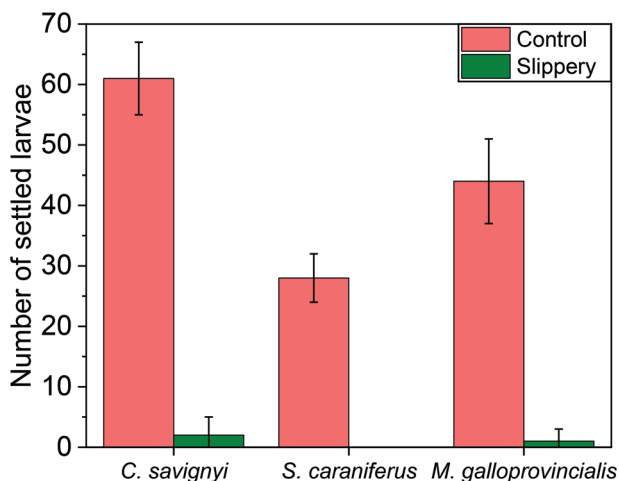


**Figure 7.** Number of marine larvae settled on uncoated Petri dishes (control) and slippery squalane-impregnated pulsed plasma poly(styrene) coated Petri dishes after 5 days. Mean values ( $n = 3$ )  $\pm$  standard error.

environments, Figure 8. Bare space (i.e., no biofouling) accounted for  $100 \pm 0\%$ ,  $83 \pm 9\%$ , and  $81 \pm 18\%$  of available space after 2, 4, and 6 weeks, respectively.

#### 4. Discussion

Aromatic–aliphatic molecular interactions between pulsed plasma poly(styrene) nanocoatings and various aliphatic group containing liquids leads to slippery behavior (water contact angle hysteresis and sliding angle values  $< 5^\circ$ ), Figure 4. This slipperiness is not due to excess liquid remaining on the surface given that there is no visible wetting ridge for water droplets resting on the liquid-impregnated surfaces, Figure S4 (Supporting Information).<sup>[88–90]</sup> The low water contact angle hysteresis values observed for decanal and 1-undecanol-impregnated uncoated PET (control) are most likely due to additional polar or hydrogen bonding interactions between the aldehyde (decanal) or hydroxyl (1-undecanol) groups respectively of these impregnation liquids and the PET substrate.<sup>[91,92]</sup> The wettability of the liquid-impregnated pulsed plasma poly(styrene) coatings can be varied from  $32 \pm 2^\circ$  (for 1-undecanol) to  $100 \pm 1^\circ$  (for hexadecane) depending on the choice of impregnation liquid, Figure 4. The use of hydrophilic slippery liquid-impregnated surfaces rather than hydrophobic surfaces provides potential scope for enhanced performance benefits relative to hydrophobic surfaces for water harvesting,<sup>[22]</sup> anti-icing,<sup>[93]</sup> and underwater oil-repellency.<sup>[94]</sup> In particular, the water contact angle value for the slippery 1-undecanol impregnated pulsed plasma poly(styrene) surface ( $32 \pm 2^\circ$ ) is lower than previously reported hydrophilic liquid-impregnated slippery surfaces.<sup>[22,93,94]</sup>

The most effective antibiofouling slippery surface in natural pond water was found to be squalane-impregnated pulsed plasma poly(styrene) yielding minimal visible fouling material after 7 days as well as displaying the lowest color change value ( $\Delta E = 1.4 \pm 1.0$ ), Figure 5. Water contact angle, water contact angle hysteresis, and sliding angle values did not change significantly for this coating or the mineral oil-impregnated surface following 7-day submersion in pond water, thereby confirming the stabil-

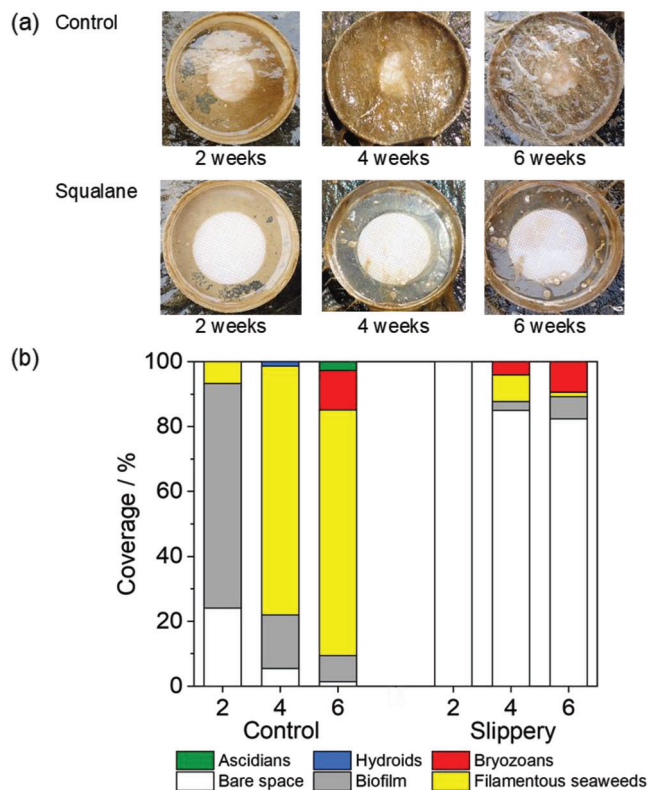


**Figure 8.** Biofouling control and squalane-impregnated pulsed plasma poly(styrene) dishes at the 2, 4, and 6-week sampling times: a) representative images (the adhesive white disk used to fix the Petri dish into the marina is on the backside of each Petri dish (below) and therefore its top views can be taken as an indication of the lack of biofouling, and b) mean percentage cover ( $n = 3$ ) of major taxonomic components of biofouling communities. Surface areas of attachment are reported in Table S3 (Supporting Information).

ity of these coatings (due to the extremely low water solubility of these liquids), Figure 6.<sup>[95,96]</sup> These observations correlate to better antibiofouling performances, Figure 5. 1-undecanol, olive oil, and rapeseed oil-impregnated pulsed plasma poly(styrene) nanocoatings acquired greater coverage of green biofouling material after 7 days of submersion in pond water compared with the control PET substrate, Figure 5. This is likely to be due to these impregnation liquids providing nutrients for adhered organisms, thereby promoting growth near the surface (greater biofouling).<sup>[97,98]</sup> Such surfaces may be useful in applications where biological adherence and growth are desirable (e.g., aquaculture bioreactors using benthic algae).<sup>[99–101]</sup>

The best performing antibiofouling slippery surface for pond water (squalane impregnated pulsed plasma poly(styrene)) was tested further using marine bioassay experiments—where it again demonstrated excellent antibiofouling performance, Figure 7. The surface-trapped oil layer acts as a physical barrier to biofouling attachment leading to interference with larvae adhesion and/or larval behavioral avoidance/rejection of the surface, Table S3 (Supporting Information). The marine antibiofouling potential of squalane-impregnated pulsed plasma polymer surfaces were further validated through ocean field trials where visibly more biofouling material accumulated on the



uncoated Petri dish sample (control) compared to the squalane-impregnated pulsed plasma poly(styrene) surfaces, Figure 8. Antifouling efficacy was maintained for at least 6 weeks in the ocean, a timeframe that matches/exceeds previous reports for slippery surfaces utilizing impregnation of natural liquids.<sup>[42]</sup> This effective timeframe has immediate potential for materials/structures with short deployment times, such as environmental monitoring equipment or sensors.<sup>[102]</sup> Other applications, for example, ship hull antifouling, require effective timeframes in the order of 1 year or longer.<sup>[103]</sup> The observed biofouling on the treated dishes comprised primarily of colonial ascidians, which expand laterally across surfaces as part of their normal growth and development.<sup>[104]</sup> Further optimization or development of methods for periodic replenishment of squalane-impregnated pulsed plasma poly(styrene) could conceivably extend efficacy to target a broader range of potential applications. Regardless, the observed antifouling efficacy is highly promising for a natural antifouling material with low collateral environmental risks.

Previously reported antibiofouling liquid impregnated textured/porous surfaces for real-world marine environments utilized fluorinated oils (e.g., Krytox). However, due to their chemical persistence and potential to bioaccumulate, there are serious environmental concerns relating to the toxic effects of these oils impacting marine life.<sup>[12,37,105–108]</sup> Alternative silicone oils considered to be more environmentally friendly, are still derived from non-renewable resources.<sup>[94,109]</sup> In contrast, the best-performing impregnation liquid in this study (squalane) is generally derived from natural plant-based sources, and widely recognized as a sustainable component, for example in cosmetics and disease management.<sup>[110,111]</sup>

Conventional slippery surface strategies based on the swelling of bulk polydimethylsiloxane (PDMS) involve time-consuming and multi-step processes including intermediary coating steps (due to the weak adhesion of the silicone material to underlying substrates).<sup>[44,47,48,51,112–114]</sup> Whilst liquid-impregnated surfaces fabricated through partial UV-grafting of silicone oil are limited to flat substrate geometries due to the inherent directionality of the UV irradiation (non-conformal). Commercial foul-release antibiofouling coatings have previously utilized natural oils (e.g., lanolin oil) but such strategies do not make use of slippery liquid interfaces and require multi-steps including primer/tie coats.<sup>[115]</sup> In contrast, the plasmachemical aromatic coatings outlined in the current study are substrate-independent, solventless, and produce minimal waste. The slippery aromatic–aliphatic intermolecular interactions combined with environmentally friendly and rapid scalable processing holds significant potential for real-world applications. For example, the use of slippery squalane-impregnated pulsed plasma poly(styrene) coatings in conjunction with bubble diffusers could provide synergistic antibiofouling benefits due to the additive cleaning effect of the bubble stream.<sup>[28,116]</sup>

## 5. Conclusions

Aliphatic liquid impregnation into pulsed plasma poly(styrene) nanocoatings produces slippery surfaces with extremely low water contact angle hysteresis and sliding angle values ( $\approx 1\text{--}2^\circ$ ). This can be attributed to stabilizing aromatic–aliphatic intermolecular interactions. Surface wettability can be tailored through care-

ful choice of impregnation liquid (water contact angle values ranging from  $30^\circ$  to  $99^\circ$ ), whilst still retaining slippery behavior. Squalane-impregnated pulsed plasma poly(styrene) nanocoating is found to be the best performing antibiofouling slippery surface in natural pond water. It also hinders the settlement of three model marine biofouling taxa larvae (*C. savignyi*, *M. galloprovincialis*, and *S. caraniferus*), and resists biofouling in the ocean for at least 6 weeks. This combination of scalable and substrate-independent pulsed plasmachemical deposition combined with natural product liquid compound impregnation offers significant potential for eco-friendly antibiofouling surfaces without causing collateral harm to the environment

## Supporting Information

Supporting Information is available from the Wiley Online Library or from the author.

## Acknowledgements

This study was supported by New Zealand Ministry of Business Innovation and Employment (grant CAWX1904) and the Royal Society (International Collaboration Award IC160021).

## Conflict of Interest

Durham University has filed an international patent application.

## Author Contributions

J.P.S.B., H.J.C., and J.M.R. devised the liquid impregnation approach for squalane-impregnated antibiofouling slippery surfaces. H.J.C. undertook preliminary plasmachemical deposition–liquid impregnation, and contact angle analysis. J.M.R. undertook plasmachemical deposition–liquid impregnation, infrared spectroscopy, atomic force microscopy, contact angle analysis, color analysis, and natural pond water testing. P.C. and G.H. carried out the marine bioassays and ocean trials. J.P.S.B. and J.M.R. jointly drafted the manuscript. All authors have given final approval for publication.

## Data Availability Statement

The data that support the findings of this study are available from the corresponding author upon reasonable request.

## Keywords

antibiofouling, eco-friendly, nanocoating, plasmachemical functionalisation, slippery surfaces

Received: April 10, 2023

Revised: July 20, 2023

Published online:

[1] I. Davidson, C. Scianni, C. Hewitt, R. Everett, E. Holm, M. Tamburri, G. Ruiz, *Biofouling* **2016**, 32, 411.

- [2] V. Vishwakarma, K. G. Saravanan, in *Polymetallic Coatings to Control Biofouling in Pipelines*, **2021**, pp. 1–13.
- [3] M. Apolinario, R. Coutinho, in *Advances in Marine Antifouling Coatings and Technologies*, Woodhead Publishing, Sawston, UK **2009**, pp. 132–147.
- [4] A. Farkas, S. Song, N. Degiuli, I. Martić, Y. K. Demirel, *Ocean Eng* **2020**, *199*, 107033.
- [5] M. P. Schultz, J. A. Bendick, E. R. Holm, W. M. Hertel, *Biofouling* **2011**, *27*, 87.
- [6] A. Lafuma, D. Quéré, *Europhys. Lett.* **2011**, *96*, 56001.
- [7] U. Bauer, W. Federle, *Plant Signal Behav* **2009**, *4*, 1019.
- [8] V. B. Wright, W. K. Poulsom, M. W. MacDonald, *An Improved Manufacture of Compounds for Water-Proofing Textile and Other Fabrics, String, Ropes, and the like, and Apparatus Therefor*, G.B. 190325000A, **1904**.
- [9] J. A. Vielle, *Improved Process for Rendering Materials Waterproof*, GB209138A, **1924**.
- [10] T. S. Wong, S. H. Kang, S. K. Y. Tang, E. J. Smythe, B. D. Hatton, A. Grinthal, J. Aizenberg, *Nature* **2011**, *477*, 443.
- [11] C. Zhang, S. Adera, J. Aizenberg, Z. Chen, *ACS Appl. Mater. Interfaces* **2021**, *13*, 15901.
- [12] R. Deng, T. Shen, H. Chen, J. Lu, H. C. Yang, W. Li, *J. Mater. Chem. A* **2020**, *8*, 7536.
- [13] Z. Qiu, R. Qiu, Y. Xiao, J. Zheng, C. Lin, *Appl. Surf. Sci.* **2018**, *457*, 468.
- [14] M. Tenjimbayashi, S. Nishioka, Y. Kobayashi, K. Kawase, J. Li, J. Abe, S. Shiratori, *Langmuir* **2018**, *34*, 1386.
- [15] S. Amini, S. Kolle, L. Petrone, O. Ahanotu, S. Sunny, C. N. Sutanto, S. Hoon, L. Cohen, J. C. Weaver, J. Aizenberg, N. Vogel, A. Miserez, *Science* **2017**, *357*, 668.
- [16] A. K. Epstein, T. S. Wong, R. A. Belisle, E. M. Boggs, J. Aizenberg, *Proc. Natl. Acad. Sci. USA* **2012**, *109*, 13182.
- [17] Z. Yang, X. He, J. Chang, C. Yuan, X. Bai, *Surf. Coatings Technol.* **2021**, *415*, 127136.
- [18] H. G. Walz, K. R. Fox, *Text. Res. J.* **1943**, *13*, 11.
- [19] S. Ozbay, C. Yucelel, H. Y. Erbil, *ACS Appl. Mater. Interfaces* **2015**, *7*, 22067.
- [20] Y. Yuan, H. Xiang, G. Liu, L. Wang, H. Liu, R. Liao, *Adv. Mater. Interfaces* **2022**, *9*, 2101968.
- [21] W. Pei, J. Li, Z. Guo, Y. Liu, C. Gao, L. Zhong, S. Wang, Y. Hou, Y. Zheng, *Chem. Eng. J.* **2021**, *409*, 128180.
- [22] X. Dai, N. Sun, S. O. Nielsen, B. B. Stogin, J. Wang, S. Yang, T. S. Wong, *Sci. Adv.* **2018**, *4*, eaaq0919.
- [23] M. Badv, S. M. Imani, J. I. Weitz, T. F. Didar, *ACS Nano* **2018**, *12*, 10890.
- [24] M. Zou, X. Zhao, X. Zhang, Y. Zhao, C. Zhang, K. Shi, *Chem. Eng. J.* **2020**, *398*, 125563.
- [25] P. A. Tsai, *J. Fluid Mech* **2013**, *736*, 1.
- [26] Y. Wang, H. Zhang, X. Liu, Z. Zhou, *J. Mater. Chem. A* **2016**, *4*, 2524.
- [27] S. J. Lee, H. N. Kim, W. Choi, G. Y. Yoon, E. Seo, *Soft Matter* **2019**, *15*, 8459.
- [28] J. M. Rawlinson, H. J. Cox, G. Hopkins, P. Cahill, J. P. S. Badyal, *Colloids Surfaces A Physicochem. Eng. Asp.* **2023**, *656*, 130491.
- [29] C. Wang, Z. Guo, *Nanoscale* **2020**, *12*, 22398.
- [30] P. Wang, D. Zhang, Z. Lu, *Colloids Surf., B* **2015**, *136*, 240.
- [31] C. S. Ware, T. Smith-Palmer, S. Peppou-Chapman, L. R. J. Scarratt, E. M. Humphries, D. Balzer, C. Neto, *ACS Appl. Mater. Interfaces* **2018**, *10*, 4173.
- [32] F. J. Peaudecerf, J. R. Landel, R. E. Goldstein, P. Luzzatto-Fegiz, *Proc. Natl. Acad. Sci. USA* **2017**, *114*, 7254.
- [33] A. M. Brzozowska, F. J. Parra-Velandia, R. Quintana, Z. Xiaoying, S. S. C. Lee, L. Chin-Sing, D. Jańczewski, S. L. M. Teo, J. G. Vancso, *Langmuir* **2014**, *30*, 9165.
- [34] G. B. Hwang, K. Page, A. Patir, S. P. Nair, E. Allan, I. P. Parkin, *ACS Nano* **2018**, *12*, 6050.
- [35] J. Bruzaud, J. Tarrade, E. Celia, T. Darmanin, E. Taffin de Givenchy, F. Guittard, J. M. Herry, M. Guilbaud, M. N. Bellon-Fontaine, *Mater. Sci. Eng. C* **2017**, *73*, 40.
- [36] K. D. Esmeryan, I. A. Avramova, C. E. Castano, I. A. Ivanova, R. Mohammadi, E. I. Radeva, D. S. Stoyanova, T. G. Vladkova, *Mater. Des.* **2018**, *160*, 395.
- [37] L. Xiao, J. Li, S. Mieszkun, A. Di Fino, A. S. Clare, M. E. Callow, J. A. Callow, M. Grunze, A. Rosenhahn, P. A. Levkin, *ACS Appl. Mater. Interfaces* **2013**, *5*, 10074.
- [38] F. Maryami, A. Olad, K. Nofouzi, *J. Ind. Eng. Chem.* **2022**, *108*, 308.
- [39] N. Keller, J. Bruchmann, T. Sollich, C. Richter, R. Thelen, F. Kotz, T. Schwartz, D. Helmer, B. E. Rapp, *ACS Appl. Mater. Interfaces* **2019**, *11*, 4480.
- [40] Z. Wang, I. T. Cousins, M. Scheringer, K. Hungerbuehler, *Environ. Int.* **2015**, *75*, 172.
- [41] C. Howell, T. L. Vu, J. J. Lin, S. Kolle, N. Juthani, E. Watson, J. C. Weaver, J. Alvarenga, J. Aizenberg, *ACS Appl. Mater. Interfaces* **2014**, *6*, 13299.
- [42] S. Basu, B. M. Hanh, J. Q. Isaiiah Chua, D. Daniel, M. H. Ismail, M. Marchioro, S. Amini, S. A. Rice, A. Miserez, *J. Colloid Interface Sci.* **2020**, *568*, 185.
- [43] A. Abdulkareem, A. E. Abusrafa, S. Zavahir, S. Habib, P. Sobolčiak, M. Lehocky, H. Pištěková, P. Humpolíček, A. Popelka, *Int. J. Mol. Sci.* **2022**, *23*, 3682.
- [44] J. Aizenberg, M. Aizenberg, P. Kim, A. Vena, *US10385181B2*, **2019**.
- [45] N. Lavielle, D. Asker, B. D. Hatton, *Soft Matter* **2021**, *17*, 936.
- [46] K. M. Kimmins, B. D. James, M. T. Nguyen, B. D. Hatton, E. D. Sone, *ACS Appl. Bio. Mater.* **2019**, *2*, 5841.
- [47] Z. Tong, L. Song, S. Chen, J. Hu, Y. Hou, Q. Liu, Y. Ren, X. Zhan, Q. Zhang, *Adv. Funct. Mater.* **2022**, 2201290.
- [48] A. B. Tesler, L. H. Prado, I. Thievensen, A. Mazare, P. Schmuki, S. Virtanen, W. H. Goldmann, *ACS Appl. Mater. Interfaces* **2022**, *14*, 29386.
- [49] P. Hu, Q. Xie, C. Ma, G. Zhang, *Langmuir* **2020**, *36*, 2170.
- [50] M. Lagerström, A. L. Wrangle, D. R. Oliveira, L. Granhag, A. I. Larsson, E. Ytreberg, *Mar. Pollut. Bull.* **2022**, *184*, 114102.
- [51] J. Aizenberg, M. Aizenberg, J. Cui, S. Dunn, B. Hatton, C. Howell, P. Kim, T. S. Wong, X. Yao, *US20150152270A1*, **2013**.
- [52] T. Gergs, C. Monti, S. Gaiser, M. Amberg, U. Schütz, T. Mussenbrock, J. Trieschmann, M. Heuberger, D. Hegemann, *Plasma Process. Polym.* **2022**, *19*, 2200049.
- [53] M. Alcaire, C. Lopez-Santos, F. J. Aparicio, J. R. Sanchez-Valencia, J. M. Obrero, Z. Saghi, V. J. Rico, G. De La Fuente, A. R. Gonzalez-Elipe, A. Barranco, A. Borrás, *Langmuir* **2019**, *35*, 16876.
- [54] M. Tenjimbayashi, R. Togasawa, K. Manabe, T. Matsubayashi, T. Moriya, M. Komine, S. Shiratori, *Adv. Funct. Mater.* **2016**, *26*, 6693.
- [55] D. B. Ninković, D. Z. Vojislavljević-Vasilev, V. B. Medaković, M. B. Hall, E. N. Brothers, S. D. Zarić, *Phys. Chem. Chem. Phys.* **2016**, *18*, 25791.
- [56] H. J. Cox, C. P. Gibson, G. J. Sharples, J. P. S. Badyal, *Adv. Eng. Mater.* **2021**, *24*, 2101288.
- [57] T. A. Miller, M. G. Mikhael, R. Ellwanger, A. Boufelfel, D. Booth, A. Yializis, *MRS Online Proc. Libr.* **1999**, *555*, 247.
- [58] A. M. Hynes, M. J. Shenton, J. P. S. Badyal, *Macromolecules* **1996**, *29*, 4220.
- [59] M. E. Ryan, A. M. Hynes, J. P. S. Badyal, *Chem. Mater.* **1996**, *8*, 37.
- [60] C. Tarducci, W. C. E. Schofield, J. P. S. Badyal, S. A. Brewer, C. Willis, *Chem. Mater.* **2002**, *14*, 2541.
- [61] A. Carletto, J. P. S. Badyal, *Phys. Chem. Chem. Phys.* **2019**, *21*, 16468.
- [62] R. Ciriminna, V. Pandarus, F. Béliand, M. Pagliaro, *Org. Process Res. Dev.* **2014**, *18*, 1110.

- [63] V. Pandarus, R. Ciriminna, F. Béland, M. Pagliaro, S. Kaliaguine, *ACS Omega* **2017**, *2*, 3989.
- [64] A. Koyasako, R. A. Bernhard, *J. Food Sci.* **1983**, *48*, 1807.
- [65] K. Liu, Q. Chen, Y. Liu, X. Zhou, X. Wang, *J. Food Sci.* **2012**, *77*, C1156.
- [66] Food and Agriculture Organization of the United Nations, Specifications for Flavoursings, Analytical Methods, **1997**.
- [67] M. Younes, G. Aquilina, L. Castle, K. H. Engel, P. Fowler, M. J. Frutos Fernandez, P. Fürst, U. Gundert-Remy, R. Gürtler, T. Husøy, P. Moldeus, A. Oskarsson, R. Shah, I. Waalkens-Berendsen, D. Wölfle, R. Benigni, C. Bolognesi, K. Chipman, E. Cordelli, G. Degen, D. Marzin, C. Svendsen, M. Carfi, C. Martino, W. Mennes, *EFSAJ* **2019**, *17*, e05675.
- [68] C. D. Ehrlich, J. A. Basford, *J. Vac. Sci. Technol. A Vacuum, Surfaces, Film.* **1992**, *10*, 1.
- [69] D. Lovering, *NKD-6000 Technical Manual*, Aquila Instruments, Cambridge, UK **1999**.
- [70] Squalane 96 111-01-3, <https://www.sigmaaldrich.com/GB/en/product/aldrich/234311> (accessed: July 2023).
- [71] C. Zhang, Y. Xia, H. Zhang, N. S. Zacharia, *ACS Appl. Mater. Interfaces* **2018**, *10*, 5892.
- [72] R. H. Dettre, R. E. Johnson, in *Contact Angle, Wettability, and Adhesion*, **1964**, pp. 136–144.
- [73] A. F. Stadler, G. Kulik, D. Dage, L. Barbieri, P. Hoffmann, *Colloids Surfaces A Physicochem. Eng. Asp.* **2006**, *286*, 92.
- [74] C. C. Chang, C. J. Wu, Y. J. Sheng, H. K. Tsao, *RSC Adv.* **2016**, *6*, 19214.
- [75] A. B. Şengül, M. M. Rahman, E. Asmatulu, *Int. J. Environ. Sci. Technol.* **2019**, *16*, 3193.
- [76] B. Pitts, M. A. Hamilton, G. A. McFeters, P. S. Stewart, A. Willse, N. Zelter, *J. Microbiol. Methods* **1998**, *34*, 143.
- [77] E. Quagliarini, A. Gianangeli, M. D'Orazio, B. Gregorini, A. Osimani, L. Aquilanti, F. Clementi, *Constr. Build. Mater.* **2019**, *199*, 396.
- [78] B. Hill, T. Roger, F. W. Vorrage, *ACM Trans. Graph.* **1997**, *16*, 109.
- [79] P. L. Cahill, J. Atalah, A. I. Selwood, J. M. Kuhajek, *PeerJ* **2016**, *4*, e1739.
- [80] P. L. Cahill, K. Heasman, A. Jeffs, J. Kuhajek, *Biofouling* **2013**, *29*, 967.
- [81] Standard Guide for Conducting Static Acute Toxicity Tests Starting with Embryos of Four Species of Saltwater Bivalve Molluscs, **2021**.
- [82] C. G. Satuito, K. Natoyama, M. Yamazaki, N. Fusetani, *Fisheries Science* **1994**, *60*, 65.
- [83] L. Gosselin, M. Sewell, *J. Mar. Biol. Assoc U K* **2013**, *93*, 1249.
- [84] K. E. Kohler, S. M. Gill, *Comput. Geosci.* **2006**, *32*, 1259.
- [85] Hexadecane, Material Safety Data Sheet No. H6703, Sigma-Aldrich Co. LLC, November 26, **2022**.
- [86] T. G. Nevell, D. P. Edwards, A. J. Davis, R. A. Pullin, *Biofouling* **1996**, *1–3*, 199.
- [87] P. Schatzberg, *J. Polym. Sci., Part C: Polym. Symp.* **1965**, *10*, 87.
- [88] S. Peppou-Chapman, C. Neto, *Langmuir* **2021**, *37*, 3025.
- [89] S. Armstrong, G. McHale, R. Ledesma-Aguilar, G. G. Wells, *Langmuir* **2020**, *36*, 11332.
- [90] C. Semperebon, G. McHale, H. Kusumaatmaja, *Soft Matter* **2017**, *13*, 101.
- [91] J. Weber, D. Petrović, B. Strodel, S. H. J. Smits, S. Kolkenbrock, C. Leggewie, K. E. Jaeger, *Appl. Microbiol. Biotechnol.* **2019**, *103*, 4801.
- [92] T. Haga, H. Ishibashi, *Sen'i Gakkaishi* **1973**, *29*, T489.
- [93] H. Y. Erbil, *Surf. Innov.* **2016**, *4*, 214.
- [94] S. Peppou-Chapman, J. K. Hong, A. Waterhouse, C. Neto, *Chem. Soc. Rev.* **2020**, *49*, 3688.
- [95] G. G. Vadas, W. G. MacIntyre, D. R. Burris, *Environ. Toxicol. Chem.* **1991**, *10*, 633.
- [96] Anonymous, *J. Am. Coll. Toxicol.* **1982**, *1*, 37.
- [97] G. Hodaifa, M. E. Martínez, S. Sánchez, *Bioresour. Technol.* **2008**, *99*, 1111.
- [98] A. Malvis, G. Hodaifa, M. Halioui, M. Seyedsalehi, S. Sánchez, *Water Res.* **2019**, *151*, 332.
- [99] H. J. Cox, I. Cooper, H. F. Kaspar, M. A. Packer, J. P. S. Badyal, *Colloids Surfaces A Physicochem. Eng. Asp.* **2022**, *639*, 128313.
- [100] P. Stévant, C. Rebours, A. Chapman, *Aquac. Int.* **2017**, *25*, 1373.
- [101] C. Peteiro, N. Sánchez, B. Martínez, *Algal Res.* **2016**, *15*, 9.
- [102] A. Whelan, F. Regan, *J. Environ. Monit.* **2006**, *8*, 880.
- [103] H. Jin, L. Tian, W. Bing, J. Zhao, L. Ren, *Prog. Mater. Sci.* **2022**, *124*, 100889.
- [104] U. Kürn, S. Rendulic, S. Tiozzo, R. J. Lauzon, *Biol. Bull.* **2011**, *221*, 43.
- [105] X. Xu, R. Chen, Y. Zheng, J. Yu, Q. Liu, J. Liu, C. Lin, J. Duan, J. Wang, *Langmuir* **2021**, *37*, 10020.
- [106] Y. Gu, L. Yu, J. Mou, D. Wu, M. Xu, P. Zhou, Y. Ren, *Mar. Drugs* **2020**, *18*, 371.
- [107] A. J. Martín-Rodríguez, J. M. F. Babarro, F. Lahoz, M. Sansón, V. S. Martín, M. Norte, J. J. Fernández, *PLoS One* **2015**, *10*, 0123652.
- [108] K. Kannan, S. Corsolini, J. Falandysz, G. Fillmann, K. S. Kumar, B. G. Loganathan, M. A. Mohd, J. Olivero, N. Van Wouwe, J. H. Yang, K. M. Aldous, *Environ. Sci. Technol.* **2004**, *38*, 4489.
- [109] D. Kansal, S. S. Hamdani, R. Ping, M. Rabnawaz, *Ind. Eng. Chem. Res.* **2020**, *59*, 12075.
- [110] S. Bom, J. Jorge, H. M. Ribeiro, J. Marto, *J. Clean Prod.* **2019**, *225*, 270.
- [111] L. H. Reddy, P. Couvreur, *Adv. Drug Delivery Rev.* **2009**, *61*, 1412.
- [112] S. Basu, B. M. Hanh, M. H. Ismail, J. Q. I. Chua, S. Narasimalu, M. Sekar, A. Labak, A. Vena, P. Kim, T. P. Galhenage, S. A. Rice, A. Miserez, *ACS Appl. Polym. Mater.* **2020**, *2*, 5147.
- [113] L. A. Bloomfield, *Int. J. Adhes. Adhes.* **2016**, *68*, 239.
- [114] Product Data Sheet and Application Guide SLIPS Dolphin, **2020**.
- [115] D. Moore, U. Scheim, K. J. Reynolds, A. L. Parry, G. Dunford, C. Price, R. A. Heath, *WO2018134124A1*, **2018**.
- [116] G. A. Hopkins, F. Gilbertson, O. Floerl, P. Casanovas, M. Pine, P. Cahill, *PeerJ* **2021**, *9*, 11323.